

## Short Communication

---

# Performance of a solid-state battery with a proton-conducting electrolyte

K. Singh

*Department of Physics, Nagpur University Campus, Amaravati Road, Nagpur-440010 (India)*

R.U. Tiwari

*Department of Applied Physics, Shri Ramdeobaba Kamala Nehru Engineering College, Katol Road, Nagpur-440013 (India)*

V.K. Deshpande

*Department of Applied Physics, VRCE, Nagpur-440011 (India)*

(Received February 15, 1993; accepted April 21, 1993)

### Abstract

An electrochemical cell of the configuration  $\text{Zn}/\text{ZnSO}_4 \cdot 7\text{H}_2\text{O}/\text{I}_2$  has given an open-circuit voltage of 1.1 V, a short-circuit current of  $>10$  mA and an energy density of  $13.8 \text{ Wh kg}^{-1}$  at a constant-current drain of  $100 \mu\text{A}$ . The details of the discharge process and the variation in the internal impedance of the cell are derived on the basis of a complex impedance analysis.

### Introduction

Because of the absence of electrode corrosion and associated liquid leakage, strong interest is being shown in solid proton conductors (SPC) for the development of fuel cells and sensors. In this regard, considerable attention has been focussed on hydrogen uranyl phosphate (HUP), potassium dihydrogen phosphate (KDP) and ammonium dihydrogen phosphate (ADP) electrolytes for a wide range of electrochemical cells that involve the transport of  $\text{H}^+$  ions [1-5]. The characteristic properties of some proton solid-state batteries have been studied by Shilton and Howe [2] and Takahashi *et al.* [6].

Several organic and metallic sulfates have been established as proton conductors, but their utility in electrochemical cell has not been explored. In the present work, we report one such attempt with the following cell configuration:  $\text{Zn}/\text{ZnSO}_4 \cdot 7\text{H}_2\text{O}/\text{I}_2$ .

Two cell systems were also been tried with oxides as cathodes. They were not, however, found to be suitable with this electrolyte. Thus, it was decided to use iodine.

## Experimental

The initial ingredients, namely zinc sulfate, metallic zinc and iodine, were obtained from E. Merck, India. The graphite powder was procured from Hindusthan Electrographite Ltd., Bhopal, India.

The electrochemical cells were fabricated by using a cathode mixture that was prepared by blending electrolyte, iodine and graphite powder in an appropriate weight ratio. A weighed amount of this mixture was pressed at  $5 \text{ ton cm}^{-2}$  to obtain a pellet of 12 mm diameter and 2 mm thickness. A weighed amount of electrolyte was pressed over the prepressed cathode at about the same pressure. Next, a known amount of zinc powder was pressed over the electrolyte surface at  $7 \text{ ton cm}^{-2}$ . Finally, the cell was assembled in holder.

The discharge characteristics for a constant current were recorded on a Keithley 617 electrometer. The impedance of the cell before, during and after the discharge was measured with a HP 4192A LF impedance analyser in the frequency range 5 to 13 MHz.

## Results and discussion

The parameters for cells with different oxide cathodes are given in Table 1. The short-circuit currents (SCC) are very low. In addition, it was observed that the cells failed within 10 days. This may be due to an incompatibility of the cathode with the electrolyte. Preliminary cells with the following configurations have been investigated:

$\text{Zn/ZnSO}_4 \cdot 7\text{H}_2\text{O/I}_2 + \text{carbon} + \text{electrolyte}$  cell (I)

$\text{Zn/Zn} + \text{ZnSO}_4 \cdot 7\text{H}_2\text{O/ZnSO}_4 \cdot 7\text{H}_2\text{O/I}_2 + \text{carbon} + \text{electrolyte}$  cell (II)

The open-circuit voltages (OCVs) of the cells are 1.21 and 1.25 V, respectively. The principle of the electrochemical cell is shown schematically in Fig. 1. The cell reactions are as follows:

TABLE 1

Cell parameters for oxide cathodes

Cell	OCV (V)	SCC ( $\mu\text{A}$ )
Zn/MnO <sub>2</sub>	1.462	10
Zn/V <sub>2</sub> O <sub>5</sub>	0.972	2
Zn/PbO	0.612	3

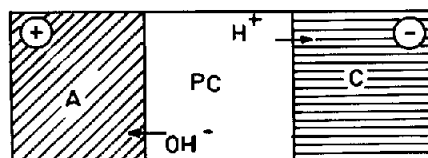


Fig. 1. Principle of all-solid-state battery. A: anode; C: cathode, and PC: proton conductor.

(i) in electrolyte:



(ii) at anode:



(iii) at cathode:



The variation of SCC with time after assembly of cells I and II is displayed in Fig. 2. It is observed that the SCC of cell I increases gradually and attains a maximum value of 10 mA after six days. Thereafter, the SCC remains constant. By contrast, the SCC of cell II rises rather sharply to a maximum of 24 mA, and then decreases rapidly. This implies that cell II cannot provide a stable performance. Hence, cell II was not subjected to further study.

The discharge characteristics of cell I under different constant-current drains are depicted in Fig. 3. As expected, the initial cell voltage decreases exponentially with time and attains a constant value within 3 h. A plateau is seen for each current drain. The drop in voltage followed by a plateau indicates complete discharge of the cell. The plateau voltage (also known as the cell operating voltage) is reproducible to within

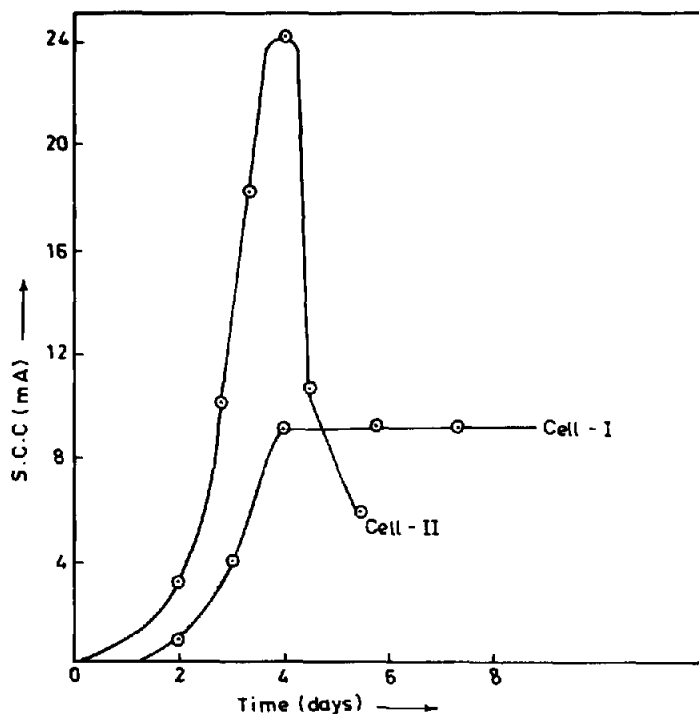


Fig. 2. Short-circuit current vs. time.

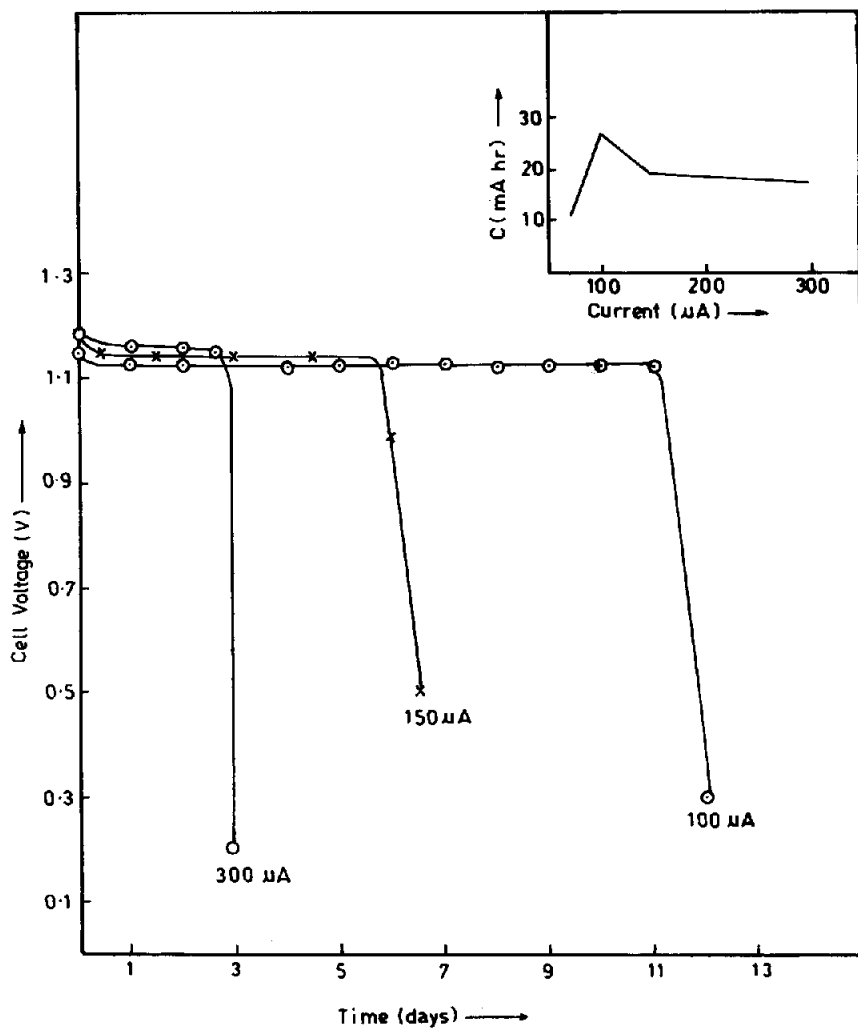


Fig. 3. Discharge characteristics of cell I.

TABLE 2

Discharge parameters for cell I

Current drain ( $\mu\text{A}$ )	100.0	150.0	300.0
Capacity (mAh)	26.40	19.80	18.90
Discharge time (h)	264.0	132.0	63.00
Operating voltage (V)	1.050	01.08	1.09
Energy density ( $\text{Wh kg}^{-1}$ )	13.86	10.69	10.3

a few mV. The discharge capacity as a function of current drain is shown in the inset of Fig. 3. The cell parameters (obtained from the discharge characteristics, Fig. 3), are summarised in Table 2. From these results, it is evident that the discharge capacity and energy density of the cell are maximum for a current drain of  $100 \mu\text{A}$ .

The complex impedance plots of cell I before, during and after discharge are presented in Fig. 4. For a particular set, there are two discernible semicircles followed

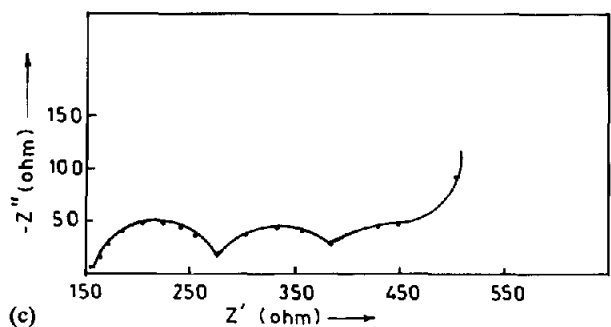
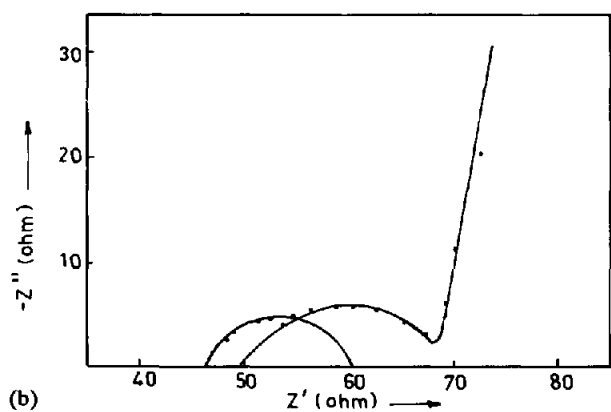
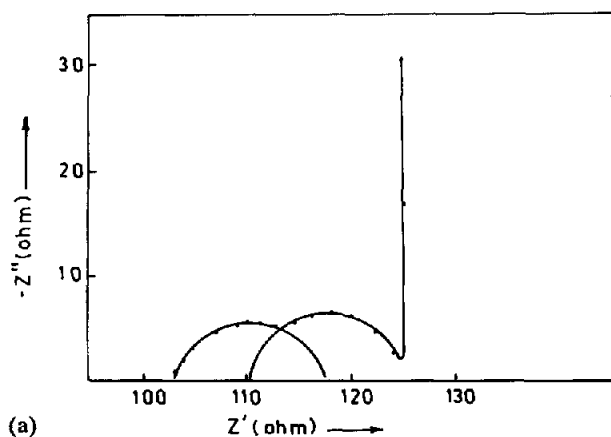


Fig. 4. Impedance diagram of cell I: (a) before; (b) during, and (c) after discharge.

by an inclined straight line in the low-frequency domain. The high-frequency semicircular arc is due to the transport of ions through the electrolyte. On the other hand, the low-frequency arc is a consequence of the diffusion of ions across the electrode/electrolyte interface. The depression in the semicircles is due to the invariance in the potential barriers of ions. The straight line at low frequencies is caused by the electrode polarization. These results are in good agreement with earlier reports [7, 8]

The internal resistance of the cell, as determined from the impedance diagrams (Fig. 4), is plotted as a function of discharge time in Fig. 5. Interestingly, the cell impedance before the discharge process is higher than that at the onset of discharge. Moreover, as discharge proceeds, the cell impedance attains a minimum and then increases. The initial decrease in the cell impedance may be due to an increase in the cell activity. The increase, followed by minimum impedance, reveals the formation of low-conducting reaction products at the electrodes.

In conclusion, it would appear that  $\text{ZnSO}_4 \cdot 7\text{H}_2\text{O}$  is a potential candidate for solid-state, proton-conducting batteries.

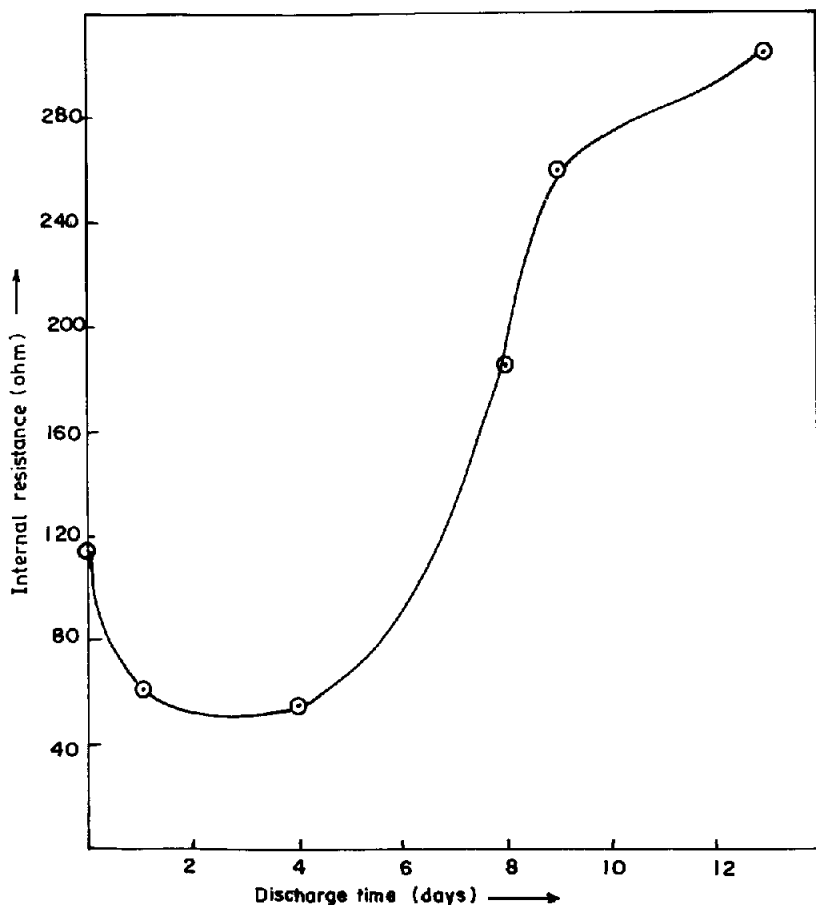


Fig. 5. Internal resistance of cell vs. discharge time.

**References**

- 1 P.E. Childs, A.T. Howe and M.G. Shilton, *J. Power Sources*, 3 (1978) 105.
- 2 M.G. Shilton and A.T. Howe, *Mater. Res. Bull.*, 12 (1977) 701.
- 3 P.E. Childs, T.K. Halstead, A.T. Howe and M.G. Shilton, *Mater. Res. Bull.*, 13 (1978) 609.
- 4 S. Chandra and A. Kumar, *Solid State Ionics*, 40/41 (1989) 255.
- 5 T. Takahashi, S. Tanase, O. Yamamoto and S. Yamauchi, *J. Solid State Chem.*, 17 (1976) 335.
- 6 T. Takahashi, S. Tanase, O. Yamamoto, *J. Appl. Electrochem.*, 10 (1980) 415.
- 7 K. Singh, S.S. Bhoga and V.K. Deshpande, in B.V.R. Chowdary and S. Radhkrishna (eds.), *Solid State Ionic Devices*, World Scientific, Singapore, 1986, p. 411.
- 8 S.P.S. Badwal, *J. Electroanal. Chem.*, 161 (1984) 75.